Sub-surface Fatigue Crack Growth at Alumina Inclusions in AISI 52100 Roller Bearings

Cerullo, Michele

Published in:
Procedia Engineering

Link to article, DOI:
10.1016/j.proeng.2014.06.274

Publication date:
2014

Document Version
Publisher's PDF, also known as Version of record

Available online at www.sciencedirect.com

ScienceDirect

Procedia Engineering 74 (2014) 333 – 338

Procedia Engineering

www.elsevier.com/locate/procedia

XV11 International Colloquim on Mechanical Fatigue of Metals (ICMFM17)

Sub-surface fatigue crack growth at alumina inclusions in AISI 52100 roller bearings

Michele Cerullo*

Technical University of Denmark, Department of Mechanical Engineering Nils Koppels Alle, 2100 Lyngby - Denmark

Abstract

Sub-surface fatigue crack growth at non metallic inclusions is studied in AISI 52100 bearing steel under typical rolling contact loads. A first 2D plane strain finite element analysis is carried out to compute the stress history in the innner race at a characteristic depth, where the Dang Van damage factor is highest. Subsequently the stress history is imposed as boundary conditions in a periodic unit cell model, where an alumina inclusion is embedded in a AISI 52100 matrix. Cracks are assumed to grow radially from the inclusion under cyclic loading. The growth is predicted by means of irreversible fatigue cohesive elements. Different orientations of the cracks and different matrix-inclusion bonding conditions are analyzed and compared.

Selection and peer-review under responsibility of the Politecnico di Milano, Dipartimento di Meccanica
Keywords: Rolling contact fatigue; AISI 52100; Inclusions; Wind Turbine; Cohesive Element

1. Introduction

It is well known that fatigue failure and mechanisms may vary a lot according to the stress level applied and that a dual step S–N curve characteristic may appear in the ultra long life regime [1–5]. At stress levels close or higher than the conventional fatigue limit, in fact, failure is more likely to be expected close to the surface of the material, while at a stress level below the fatigue limit, fatigue failure usually occurs at small internal defects. The latter mechanism becomes dominant in the very high cycle fatigue (VHCF), that is to say for a number of cycles bigger than 10^{11}, while a coexistence of surface and subsurface failures is present in the range between 10^6–10^9 cycles [2–6].

Subsurface failure is usually dominated by crack initiation, which is strongly influenced by the features and the defects in the microstructure [6]. Inclusions or pores may act as stress concentration sites, and cracks may nucleate around these defects and then propagate to the surface. Sometimes microstructural changes are observed around inclusions, where a fine granular area, known as fish-eye, may develop for low stress amplitudes [3,4,7–9].

Traditional approaches against rolling contact fatigue (RCF) consist in designing with respect to a maximum Hertzian pressure [10], or by means of multiaxial fatigue criteria, as the Dang Van criterion [11], which has been widely used for decades [12]. Though these approaches may be more practical, they somehow neglect the complexity of the VHCF mechanisms. Service life in the VHCF regime is in fact strongly influenced by the presence of small inclusions, and therefore other design criteria have been proposed, as calculations based on the stress intensity factor (SIF) [13] or by means of the Murakami's method [14].

The study of fatigue failure in the high and very high cycle regime is of extreme importance in those applications, as for example wind turbine roller bearings, where any failures of the mechanism reflect in down-time costs which

*Corresponding author. Tel.: +45 45254278; fax: +45 45931475; mcer@mek.dtu.dk.

Selection and peer-review under responsibility of the Politecnico di Milano, Dipartimento di Meccanica
doi:10.1016/j.proeng.2014.06.274

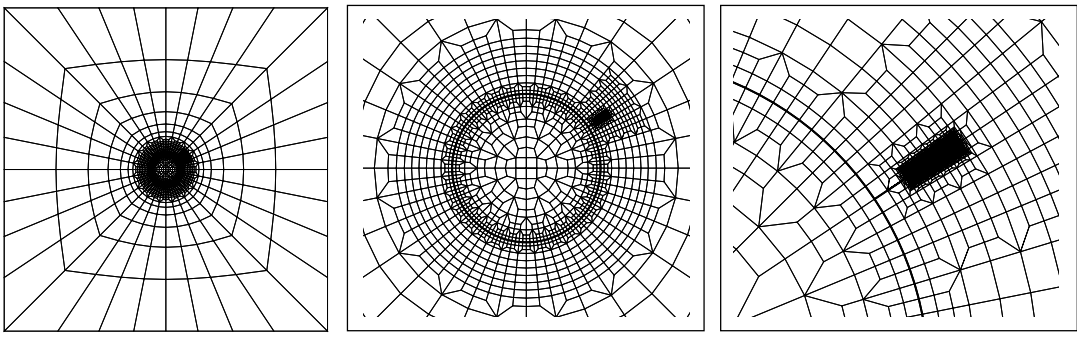

(a) (b) (c)

Fig. 1: Mesh used for the calculations at full scale (a) and at different levels of detail (b)-(c). In (c) the mesh around the crack is shown. $\theta = 30°$

.

have to be minimized [15,16]. For these mechanical systems, in fact, a service life as long as 20 years, equivalent to more than 10^{11} cycles, is expected [17], but failure sometimes occurs long before this design life.

In this work rolling contact fatigue at an interior Al_2O_3 inclusion in a AISI 52100 roller bearing is investigated. The study assumes that a small crack has already nucleated in the matrix, close to the inclusion, and therefore the crack initiation process and time are neglected. The focus is here on the influence of the inclusion depth and on the angle of the crack relative to the rolling surface. The characteristic rolling contact stress history is computed in a previous work [18] and is applied here as periodic boundary conditions. The fatigue crack growth is modelled by irreversible cohesive elements [19] and the results are compared in terms of number of cycles.

2. Problem formulation

In [18] a plane strain finite element model of a bearing ring in contact with a roller was investigated, substituing the roller with the equivalent Hertzian load, and a characteristic rolling contact stress history was recorded, at the depth of maximum Dang Van damage factor.

The macroscopic stress history $\Sigma_{ij}(t)$ is here imposed as periodic boundary condition to a unit cell of AISI 52100, in which a circular inclusion of Al_2O_3 is embedded. A straight initial crack starting from the inclusion-matrix interface is present in the matrix, at a fixed angle for each calculation. Fatigue crack growth is modelled by means of cohesive elements alligned along a straight path. Thus, the crack is assumed to grow without kinking.

In order to decrease the computational expense, the stress history, initially recorded in [18] using 179 points. It has been found that an interpolation using only 12 points gives sufficient accuracy. Between each time steps, a number of 200 increments has been used for the calculations.

The cohesive elements are described by the Roe-Siegmund irreversable constituive law [19] that models the fatigue crack growth incorporating a damage parameter, D, in the traction–separation law. When this parameter, that initially in the undamaged element is set to zero, reaches the limit value of one, the cohesive element has failed in that integration point. A penalty method is here used to ensure that the periodic boundary conditions are respected (see [20] for details). A detail of the mesh used in the finite element computations is shown in Fig. 1.

According to the the Roe-Siegmund model the traction separation law is given by:

$$\begin{aligned} T_n &= \sigma_{max,0} e \exp\Big(-\tfrac{\Delta u_n}{\delta_0}\Big)\Big\{\tfrac{\Delta u_n}{\delta_0}\exp\Big(-\tfrac{\Delta u_t^2}{\delta_0^2}\Big) + (1.0-q)\tfrac{\Delta u_n}{\delta_0}\Big[1.0-\exp\Big(-\tfrac{\Delta u_t^2}{\delta_0^2}\Big)\Big]\Big\} \\ T_t &= 2\sigma_{max,0} e q \tfrac{\Delta u_t}{\delta_0}\Big(1.0+\tfrac{\Delta u_n}{\delta_0}\Big)\exp\Big(-\tfrac{\Delta u_n}{\delta_0}\Big)\exp\Big(-\tfrac{\Delta u_t^2}{\delta_0^2}\Big) \end{aligned} \tag{1}$$

while the current cohesive strenghts are defined as

$$\begin{aligned} \sigma_{max} &= \sigma_{max,0}(1-D) \\ \tau_{max} &= \tau_{max,0}(1-D) \end{aligned} \tag{2}$$

The damage rate constitutive law is

$$\dot{D}_c = \frac{|\Delta\dot{\overline{u}}|}{\delta_\Sigma}\Big[\frac{\overline{T}}{\sigma_{max}} - C_f\Big]H(\Delta\overline{u} - \delta_0) \qquad \dot{D}_c \geq 0 \tag{3}$$

where $\overline{T}$ is the effective traction and $\Delta\overline{u}$ the accumulated separation (see [19]). A value of $\delta_\Sigma = 4\,\delta_0$ was choosen for this study. The parameter C_f represents the ratio between the cohesive endurance limit and the initial undamaged cohesive normal strenght:

$$C_f = \frac{\sigma_f}{\sigma_{max,0}}, \;\; C_f \in [0, 1] \tag{4}$$

Once an element has failed ($D = 1$), it still retains some strenght in compression, if $\Delta u_n < 0$, such that overlap is penalized

$$T_{n,compr} = \alpha\sigma_{max,0} e \exp\Big(-\frac{\Delta u_n}{\delta_0}\Big)\frac{\Delta u_n}{\delta_0} \quad , T_t = 0 \quad if \;\; \Delta u_n < 0, \;\; D = 1 \tag{5}$$

The penalty factor α was choosen to be $\alpha = 10$. No friction term was here introduced in the equations that describe the contact condition, see Eq.(5).

The periodic cell has a lenght of $l = 200\,\mu m$, while the radius of the inclusion is $R = 0.05\,l$, which is a typical value for Al_2O_3 in these steels [14]. Though the actual shape of the inclusion in the reality can be also different, e.g. ellipsoidal, it was here modelled as perfect circular.

The crack is assumed to have an initial lenght a_0 and to be inclined at an angle θ with respect to the rolling direction. One initial crack lenght, $a_0 \approx 1.5\,\mu m$ was considerd, while the angle θ that defines the angular position of the crack with respect to rolling direction is varied between 0° and 120°. The maximum allowed crack length is $a_0 \approx 2.97\,\mu m$: if the crack reaches this lenght, the computations are automatically stopped. Three different cases are considered, "CRC", "INT" and "POR". The first two assume an inclusion in the matrix, while the latter assumes a pore. The CRC case reflects the case of a crack in the matrix that is perfectly bonded to the inclusion. The two crack tips are here both in the matrix. The INT case models the case where the matrix–inclusion interface is flexible and therefore cohesive elements are used here along the interface, though they are not allowed to fail. The crack in this case has a crack tip in the matrix and a crack tip on the inclusion. The value of $E_i/E_m = 1.852$ has been used as ratio between the inclusion and the matrix Young's modulii, while the Poisson's ratio of the alumina, ν_i, is taken to be 0.25. The matrix has a Young's Modulus $E_m = 210\;GPa$ and a Poisson's ratio $\nu_m = 0.3$. The material behaviour in both the inclusion and the matrix is modelled as linear elastic.

3. Results

3.1. Test case

A test case with a cracked panel subjected to $R = \sigma_{min}/\sigma_{max} = 0$, $\sigma_{max} = 100\;MPa$ is first studied, in order to evaluate the Siegmund's model parameters δ_0, σ_{max0} and C_f. The parameter q was set equal to 0.429, so that the maximum normal and shear stresses are the same. Furthermore, the fatigue limit C_f was set equal to 0.005. This choice is justified on one hand by the need to reduce the set of parameters to be varied in the test case computations. Fixing the value of C_f in fact, δ_0 and σ_{max0} were the only two others parameters to be fitted. The value of C_f choosen, which appears small, is justified in the prospective of modeling the VHCF regime, where even small values of the stress imposed, below the conventional fatigue limit, may cause failure. Though these preliminaries computations were set to fall into the low cycle regime, this seemed the best choice. Furthermore is worth to notice that the test case was carried out assuming long–crack theory even though the subsequent case assumed cracks in the order of a micron.

A Paris law with $C = 11 \cdot 10^{-10}$ and $m = 4.05$ was fitted with the set of parameters $\delta_0 = 0.5\;\mu m$, $\sigma_{max0} = 21000\;MPa$ and $C_f = 0.005$, see Fig. 2. The resulting crack growth rate is in the order of $10^{-6}\;m/cycle$, with an initial $\Delta K_I \approx 5.63\;MPam^{0.5}$ ($DK_{th} = 5\;MPam^{0.5}$). This crack growth rate is at least 3 order of magnitude higher than what expected for this material for cracks in vacuum [21], but it was here chosen to have a qualitative understanding of the crack propagation under rolling contact, rather than trying to simulate the exact number of cycles to failure which is,

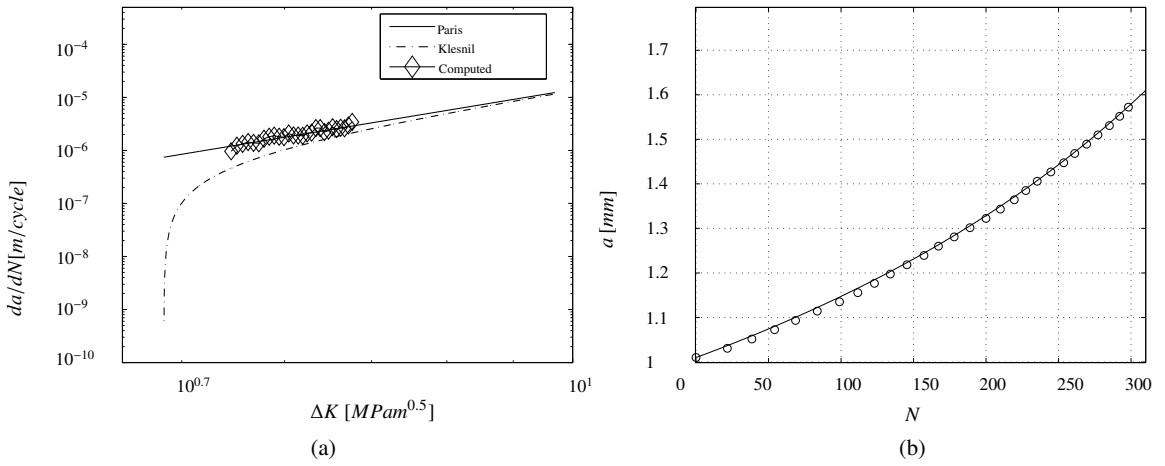

Fig. 2: (a) Fatigue crack growth rate versus the stress intensity range for the test case and (b) corresponding crack lenght – cycles curve.

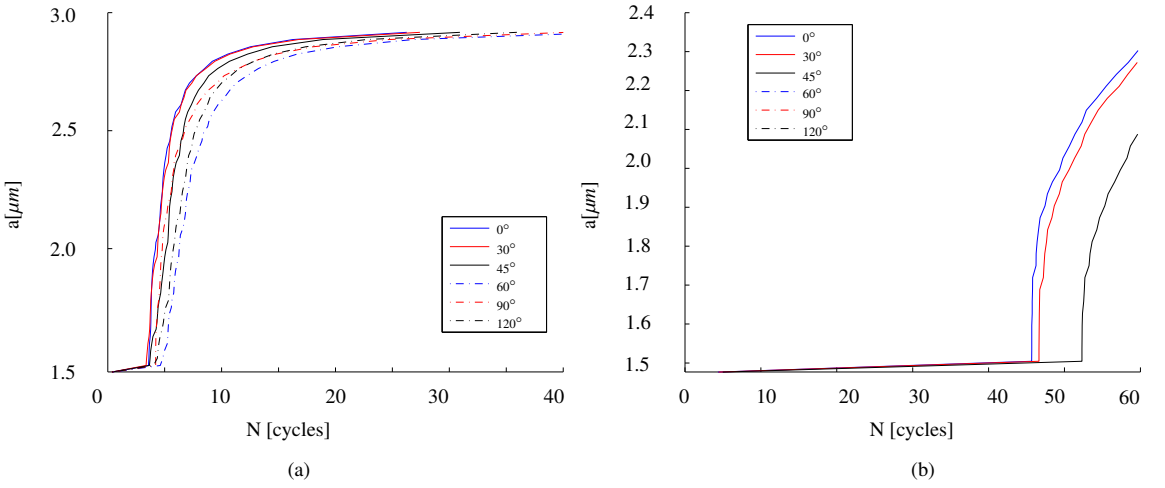

Fig. 3: Crack lenght evolution for "CRC" case, assuming (a) $\delta_0 = 0.05\ \mu m$ and (b) $\delta_0 = 0.5\ \mu m$. In (b) only cracks with angles between 0° and 45° propagated within 60 cycles.

on the other hand, practically unfeasible in the giga cycle regime. The parameters for the cohesive law were thus used in the following calculations to study crack propagation in the inclusion–matrix unit cell.

3.2. Rolling contact results

Results in terms of crack lenght and number of cycles applied are shown in Figs. 3-4. From Fig. 3 ("CRC")is clear that a to a smaller value of $\delta_0 = 0.5\ \mu m$, i.e. a stiffer cohesive traction-separation law, corresponds a quicker propagation of the crack, regardless of the angle. The cracks with angles between 0° and 30° have the fastest propagation (Fig.3a), though differences with other angles are small. This seems to be confirmed also in Fig. 3b, where only angles smaller than 45° propagated within 60 cycles. Figures 4a-b, that refer to cases INT and POR, respectively, show the same trend related to the angle of the crack: the crack growth is slightly slower than the case CRC, and only the crack oriented at 90° seems to propagate considerably slower. All the results showed "S" shaped curves and further investigations are being carried out. The author believes that this may be due to the small size of the region where the cohesive elements are placed.

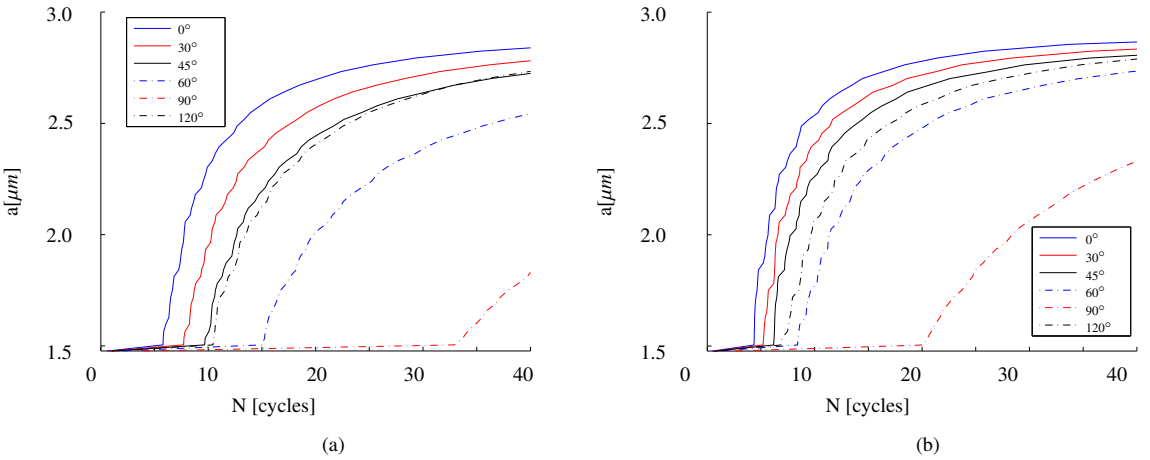

Fig. 4: Crack lenght evolution for (a) "INT" and (b) "POR" cases. $\delta_0 = 0.5\ \mu m$.

4. Conclusions

Fatigue crack growth under a typical rolling contact stress history has been investigated in this work, for different crack angles, for different inclusion-matrix conditions and for the case of a pore. Results show that crack angles between 0° and 45° propagate faster, but further investigations are suggested.

Acknowledgements

The work is supported by the Strategic Research Center "REWIND - Knowledge based engineering for improved reliability of critical wind turbine components", Danish Research Council for Strategic Research, grant no. 10-093966.

References

[1] Y. Murakami, T. Nomoto, T. Ueda. Factors influencing the mechanism of superlong fatigue failure in steels. Fatigue Fract. Eng. Mater Struc 22 (1999) 581–590.
[2] S. Nishijima, K. Kanazawa. Stepwise S–N curve and fish-eye failure in gigacycle fatigue. Fatigue Fract. Eng. Mater Struc 22 (1999) 601–607.
[3] K. Shiozawa, L. Lu, S. Ishihara. S–N characteristics and subsurface crack initiation behaviour in ultra-long life fatigue of a high carbon-chromium bearing steel. Fatigue Fract. Eng. Mater Struc 24 (2001) 781–790.
[4] K. Shiozawa, Y. Morii, S. Nishino, L. Lu. Subsurface crack initiation and propagation mechanism in high-strength steel in a very high cycle regime, Int. Journal of Fatigue 28 (2006) 1521–1532.
[5] T. Sakai, M. Takeda, K. Shiozawa et al.. Experimental evidence of duplex S–N characteristics in wide life region for high strength steels, in: Fatigue 99, Vol. I. (edited by X.R. Wu and Z.G. Wang). Higher Education Press, pp. 573–578.
[6] K. S. Chan. Roles of microstructure in fatigue crack initiation, Int. Journal of Fatigue 32 (2010) 1428–1447.
[7] M. -H. Evans, White structure flaking (WSF) in wind turbine gearbox bearings: effects of 'butterflies' and white etching cracks (WEC). Journal of Materials Science and Technology 28 (2012) 3–22.
[8] M. -H. Evans, A. D. Richardson, L. Wang, R. J. K. Wood, Serial sectioning investigation of butterfly and white etching crack (WEC) formation in wind turbine gearbox bearings (2013) http://dx.doi.org/10.1016/j.wear.2012.12.031.
[9] A. Grabulov, R. Petrov, H. W. Zandbergen. ESBD investigation of the crack initiation and TEM/FIB analysis of the microstructural changes around the cracks formed under Rolling Contact Fatigue. International Journal of Fatigue 32 (2010) 576–583.
[10] T.A. Harris, M.N. Kotzalas. Rolling bearing analysis, Boca Raton (FL) CRC Press; 2007.
[11] K. Dang Van, G. Cailletaud, J.F. Flavenot et al..Criterion for high cycle fatigue failure under multiaxial loading, in: Biaxial and Multiaxial fatigue. Mechanical Engineering Publications, London: pp 459–478, 1989.
[12] S. Foletti, S. Beretta, M. G. Tarantino. Multiaxial fatigue criteria versus experiments for small crack under rolling contact fatigue, Int. Journal of Fatigue 58 (2014) 181–182.
[13] L. Hua, S. Deng, X. Han, S. Huang. Effect of material defects on crack initiation under rolling contact fatigue in a bearing ring, Tribology International 66 (2013) 315–323.

[14] Murakami Y. Metal Fatigue: Effects of Small defects and Nonmetallic Inclusions. Elsevier, Oxford, 2002 pp.5–8.
[15] Spinato F, Tavner PJ, van Bussel GJW, Koutoulakos E, Reliability of wind turbine subassemblies. IET Renew Power Gener 2009; vol 3 4: 387?401.
[16] Yang M, Chengbing H, Xinxin F. Institutions Function and Failure Statistic and Analysis of Wind Turbine. Physics Procedia 2012; 24:25?30.
[17] Ragheb A, Ragheb M. Wind turbine gearboxes technologies, Proceedings of the 1st International Nuclear and Reneawble Energy Conference, Amman, Jordan, 21-24 March 2010.
[18] M. Cerullo, Application of Dang Van criterion to rolling contact fatigue in wind turbine roller bearings under elastohydrodynamic lubrication conditions, P I Mech eng C-J Mec Prepublished December 20th 2013, DOI 10.1177/0954406213516946
[19] K. L. Roe, T. Siegmund. An irreversible cohesive zone model for interface fatigue crack growth simulation, Engineering fracture mechanics 70 (2003) 70:209–232.
[20] V. Tvergaard. Effect of stress-state and spacing on voids in a shear-field. International Journal of Solids and Structures, vol 49, no. 22, pp. 3047-3054.
[21] S. Stanzl-Tschegg, B. Schonbauer. Near-treshold fatigue crack propagation and internal cracks in steel, Procedia Engineering 2 (2010) 1547–1555.
[22] M. Cerullo, V. Tvergaard. Micromechanical study of the effect of inclusions on fatigue failure in a roller bearing. Paper sumbitted.